Advances in Reliability, Safety and Security, Part 3 – Kołowrocki, Dąbrowska (eds.)
 ISBN 978-83-68136-15-9 (printed), ISBN 978-83-68136-02-9 (electronic)

Advances in Reliability, Safety and Security

ESREL 2024
Monograph Book Series

Copula Based Bayesian Networks For Hydrodynamic Load Estimation On Offshore Aquaculture Systems

Rieke Santjer[a,b], Patricia Mares-Nasarre[c], Ghada El Serafy[a,b], Oswaldo Moreales-Nápoles[c]

[a]*Marine and Coastal Systems, Deltares, Delft, The Netherlands*
[b]*Deft Institute of Applied Mathematics, Delft University of Technology, The Netherlands*
[c]*Hydraulic Structures and Flood Risk, Delft University of Technology, Delft, The Netherlands*

Abstract

Seaweed aquaculture, particularly the cultivation of Saccharina latissima, presents a promising solution for protein and energy demands. Offshore locations for example in the North Sea have a huge potential for aquaculture, however, the harsh offshore conditions require a thorough understanding of structural loads. This study makes use of a copula-based Bayesian Network approach to assess wave and current induced loads on the mooring lines independent from the remaining seaweed cultivation structure located in the German North Sea. A three-dimensional hydrodynamic model is used to extract five variables to describe wave and current behaviour. A k-means clustering algorithm is used to account for different wave and current appearances. For each of these clusters, copula-based Bayesian networks (BN) are constructed, which represent the probabilistic dependence between the variables. Validation of these BN's is done using d-calibration score and in-sample simulations. From each BN, samples are drawn for the relevant variables. Based on these, the loads on the mooring lines due to wave and current flows are calculated via the Morison equation. Reasonable loads below 1.8 kN per cluster are obtained. Copula-based Bayesian Networks provide a robust approach for modelling uncertainty in extreme conditions in this study. Future research aims to refine load estimations, consider dynamics, and explore different dependence structures using vine-copula models.

Keywords: mooring line, morison equation, waves, currents, Bayesian Network, Gaussian copula

1. Introduction

Seaweed aquaculture has emerged as a potential solution to address the demand for proteins and energy (Kerrison et al., 2015). Neither does it require freshwater, nor will it contribute to the land use competition. The species Saccharina latissima proved to be well suited (Geisler et al., 2018; Maar et al., 2023.) and is characterised by high growth rates and biomass yield potentials (Araújo et al., 2021). Additionally, seaweed has the ability to extract nutrients and carbon from the seas (Yong et al., 2022, Boderskov et al., 2023). However, the competition at sea, especially close to the shore, is continuously increasing. Thus, aquaculture is moving further offshore. Especially the North Sea has a huge potential for aquaculture cultivation. Offshore cultivation structures, however, face a harsh environment. Despite the feasibility of offshore cultivation (Buck et al., 2008; Gagnon and Bergeron, 2017), further knowledge is needed to understand the loads on these structure in extreme events.

Due to the harsh environment, significant impacts on the structure are expected, which leads to large forces acting on the structure, especially on the mooring lines. According to Stevens et al. (2007) and Feng et al. (2021), the biomass acts as the main drag element. Also, the angle of waves in relation to the structure orientation is crucial, while the upper buoy configuration can be neglected (Feng et al., 2021). In this study, a simplified approach is described to assess the loads on the mooring line due to wave and current impacts,

independent from the remaining structure. This study concentrates on the location of the FINO3 research platform in the German North Sea (see Section 2). An ecological assessment of cultivating the seaweed species Saccharina latissima has been previously conducted (Santjer et al., 2023).

In order to assess the loads on the mooring lines, data is used from a three-dimensional hydrodynamical model for a duration of 5 years, which is further described in Section 2. Five variables are selected to calculate the forces due to wave and current velocities by using the Morison equation (see Section 3).

To account for single components of the wave and current appearance at the selected location, a clustering algorithm is applied (see Section 3.1). For each of these clusters, a copula-based Bayesian Network (BN) is set-up in order to build a multidimensional probability distribution (see Section 4). Copula models are used to describe the joint distribution between variables (Joe, 2015). For the BN's, gaussian copula models are used to build the dependence structure between variables. Two techniques are applied in Section 4.4 to validate the models. Finally, the exceedance probability curve of calculated loads is presented in Section 5.

2. Case study

In this study, a longline structure to cultivate the seaweed species Saccharina latissima at the location of the FINO3 research platform (55.195°N, 7.1583°E) is used as a case study. The platform is subjected to severe offshore conditions because of its exposed location (marked by a star in Figure 1 (a)). The water depth at this location is 23 m. Here, initial steps are taken to assess the loads on a structure. An overview of such a longline structure for the seaweed cultivation is given in Figure 1 (b) (Strothotte et al., 2021). The structure is characterised by several floating elements connected by ropes, where the main rope is called backbone, mooring lines and anchors (Plew et al., 2005; Stevens et al., 2008). The seaweed is cultivated between the single buoys in the middle part of the structure. The angle of the structure orientation is 315° (SW to NE).

To assess the loads on the mooring lines caused by waves and currents, data of these variables at the location of interest is necessary. These loads are assessed on the mooring lines independent from the remaining structure and the growing biomass. Current velocities in x- and y-directions (c_X and c_Y, respectively) at a depth of 3 m (see Figure 1 (b)) are computed using the three-dimensional Dutch Continental Shelf Model – Flexible Mesh (3D DCSM-FM) (Zijl et al., 2023). This model makes use of the software D-Flow Flexible Mesh (D-Flow FM) (Deltares, 2023). The domain covered by the model can be seen in Figure 1 (a) (specifically from 17°W to 13°E and 43°N to 64°N).

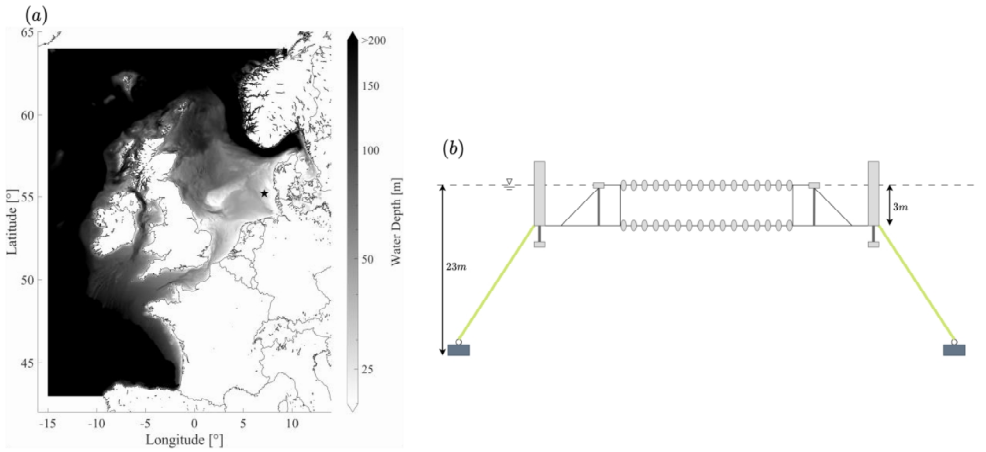

Fig. 1. (a) Model domain of the 3D-DCSM FM model, showing the water depth in the area.
The black star indicates the location of the FINO3 research platform, which is used for this case study.
(b) Example set-up of a seaweed structure according to the one tested
at the location of the FINO3 research platform (Strothotte et al., 2021).

Building on this model, the third-generation spectral wave model SWAN (Simulating Waves Nearshore, (Booij et al., 1999)) is used. It solves shallow water processes and computes significant wave height H_S, peak wave period T_P and the angle θ of the waves.

Data for the growth season of the species Saccharina latissima is extracted from both models, September until May, for 5 consecutive years (2013 until 2017). The current velocity data has a resolution of 10 minutes, while the wave data of the SWAN model has an hourly resolution.

3. Modelling approach

In the Section above, the selected variables from the hydrodynamic model are mentioned, which are necessary to calculate the loads on the mooring lines due to wave and current impact.

Next, the methodology for this paper is described.

- The variable H_S is dominant as it is the main driver for particle velocities close to the surface. Therefore, daily maxima of H_S are selected together with the corresponding T_P and θ. Within a time window of 8 hours, the maxima of c_X and c_Y are selected.
- Next, a clustering procedure is performed to identify environmental patterns (such a grouping on marine conditions according to different weather types was performed by Camus et al. (2019)) and to capture specific relations more accurately.
- Different BN's per cluster are built. The structure differs per group and is based on the observed Spearman's rank correlations between the variables (Spearman, 1987).
- The assessment of the fit of each BN is done using d-calibration score (Moráles-Napoles et al, 2013; Moráles-Napoles et al., 2014) and in-sample simulations. For the in-sample simulations, half of the data points are used to build the BN, while the remaining data points are used for validation (see Section 4.6).
- Using the BN's, samples for each variable are derived per cluster. Using linear wave theory (Airy, 1845), the horizontal velocity of the surface waves is calculated. The in-line component of the flow velocity of both, waves and currents, with respect to the orientation of the structure is determined at a depth of 3 m, as this is the main growth depth of the seaweed species (see Figure 1 (b)).
- Finally, the force on the mooring lines (marked in green in Figure 1 (b)) induced by wave and current flows is calculated via the Morison equation (see Section 3.4) and presented in the form of exceedance probabilities. The sampled flow velocities of both, waves and currents, are used to calculate the forces.

3.1. Clustering

Wave and current characteristics at the location of the FINO3 research platform in the offshore environment of the North Sea are compositions of several environmental components. To identify those patterns and to capture characteristics more accurately, groups are identified via the k-means++ algorithm (Arthur and Vassilvitskii, 2007). K-means is a popular unsupervised machine-learning technique which partitions data into groups. This algorithm maximises the distances between the centroids of each cluster while minimising the intra-cluster variation. This intra-cluster variation is assessed via the Euclidean distance of each point to the closest centroid. The algorithm is initialised by randomly selecting a set of points within the data as centroids. Thus, the solution of the algorithm depends on such initial selection and may lead to spurious solutions. To prevent this, the k-means++ algorithm is used, which is an extension of the k-means algorithm where the initial centroids are selected as follows:

- Choose initial centre c_1 uniformly at random from the set of points χ.
- Choose next centre c_i, selecting $c_i = x' \in \chi$ with probability $\frac{Z(x')^2}{\sum_{x \in \chi} Z(x)^2}$, whereas $Z(x)$ is the shortest distance from data point x to the closest centre.
- Repeat step above until a total of k centres $K = \{c_1, \dots, c_k\}$ is chosen.
- For each $i \in \{1, \dots, k\}$, set the cluster K_i to be the set of points in χ that are closer to c_i than they are to c_j for all $i \neq j$.
- For each $i \in \{1, \dots, k\}$, set c_i to be the centre of mass of all points in K_i: $c_i = \frac{1}{|c_i|} \sum_{x \in C_i} x$.
- Repeat the two steps above until K no longer changes.

Here, the implementation in Scikit-learn Python package is used (Pedregosa et al. 2011).

The main hyperparameter of the k-means algorithm is the number of clusters, which is chosen here using the elbow method. For this, the k-means++ algorithm is applied several times for different numbers of clusters, k, and the sum of squared errors (SSE) is calculated. By increasing k, the SSE decreases. SSE can be plotted against the number of clusters. The point where the curve starts to bend is the so-called elbow point and indicated a reasonable trade-off between SSE and the number of clusters.

3.2. Copula model

The BN's used in this study are based on bivariate Gaussian copulas to describe the dependence between variables. Copulas are joint multivariate distributions with uniform marginal distributions in [0,1]. For the bivariate case, copulas are defined as

$$H(x, y) = C(F(x), G(y)), \tag{1}$$

where $H(x, y)$ is a joint distribution with marginals $F(x)$ and $G(y)$ and C is a copula in the unit square $I^2 = ([0,1] \times [0,1])$. Equation (1) is satisfied for all $(x, y) \in \mathbb{R}^2$ (Joe, 2015).

3.3. Copula-based Bayesian Networks

Bayesian Networks are high-dimensional probability distributions composed by directed acyclic graphs (DAG). Each node in the graph represents a random variable, described using the empirical distribution function, while the arcs between the nodes describe the probabilistic dependence between the variables. The joint probability density over a set of variables is represented by defining conditional probability functions for each variable (child), accounting for its immediate preceding variables (parents) (Hanea et al., 2006). The Gaussian bivariate copula is used to describe the probabilistic dependence between variables as it presents computational advantages (Mendoza-Lugo et al., 2022).

Bayesian Networks have for example been applied to predict injuries and drowning due to shore breaking waves and rip currents (de Korte et al., 2021). More specifically, copula-based Bayesian Networks have for example been applied to model marine conditions for different weather conditions (Camus et al., 2019) or to model extremes of wave and wind variables (Mares-Nasarre et al., 2023).

In this study, the BN's are implemented using the Python library BANSHEE (see Paprotny et al. (2020) and Koot et al. (2023) and for the MATLAB implementation see Mendoza-Lugo and Morales-Nápoles (2023)).

3.4. Load calculation via Morison equation

To estimate the in-line forces on the mooring lines caused by wave and current flow velocities, the Morison equation is used (Morison et al., 1950). The Morison equation is an empirical formula to assess loads on slender, cylindrical and fixed structures, by the influence of water particle velocity and acceleration. Thus, in this approach, it is assumed that the mooring lines are held fixed. To calculate the loads, the Morison equation consists of two terms: the drag force f_D and inertia force f_I, which is the sum of the hydrodynamic mass force and Froude-Krylov force (Sumer and Fredsøe, 2006). It can be defined per unit elemental length as

$$f = f_I + f_D = \rho C_M \frac{\pi D^2}{4} \dot{u} + \frac{1}{2} \rho C_D |u| u, \tag{2}$$

where ρ = water density, D = diameter of the structure, u is the particle velocity in horizontal direction and $\dot{u}$ is the horizontal acceleration of the water particle. C_M and C_D, inertia and drag coefficient, respectively, are empirical constants (Chakrabarti, 2005; Sumer and Fredsøe, 2006). According to Sumer and Fredsøe (2006), the inertia induced force f_I can be neglected, if the Keulegan-Carpenter number is greater than around 20 to 30, which is defined as

$$KC = \frac{U_m T_p}{D}, \tag{3}$$

where U_m is the maximum flow velocity and T_p is the period of the oscillatory flow, which is here set to the peak wave period. In this study, due to the small diameter of the ropes D, the KC number is in the order of 10^2 and thus, the force calculated via the Morison equation can be simplified to the drag force f_D.

The drag force is induced by the flow velocities and thus, the flow accelerations can be neglected.

4. Building the probabilistic model

4.1. Identifying and clustering extremes

As described above in Section 3, 5 variables are selected, of which H_S is selected as dominant. Thus, daily maxima of H_S is sampled together with the concomitants of the other variables as the maximum within a time window of 3 hours. For the growth seasons between the years 2013 and 2017, this results in 1191 data points per variable. An overview of the data is shown in Figure 2. Applying the k-means++ clustering algorithm described

in Section 3.1, 7 clusters are identified with a variable amount of data points between 53 and 326. In this Section, the results of the 6th cluster are presented as an example, as the amount of data points is comparably high (specifically 285 data points). Other clusters were quantified similarly to cluster 6.

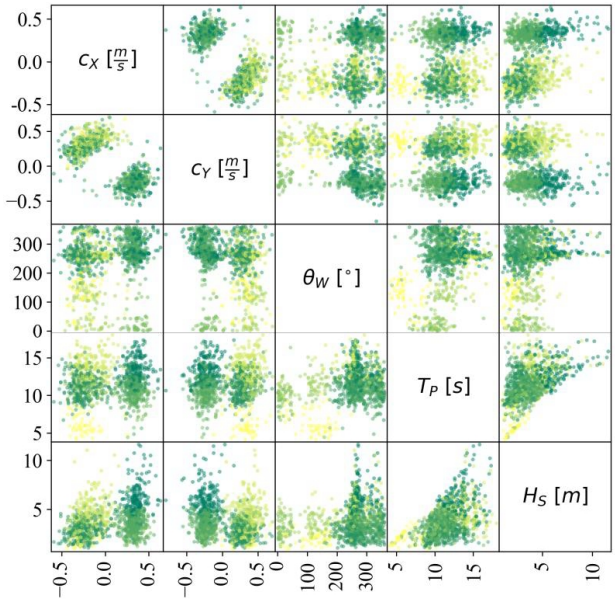

Fig. 2 Overview of daily extremes for surface waves (H_S, T_P, θ) and currents (c_X, c_Y) of available data from the hydrodynamic models, where the different colours indicate the data belonging to the 7 different clusters.

4.2. Empirical rank correlation matrix

Spearman rank correlation coefficients (r) are calculated (Spearman, 1987) for data within each cluster to assess the dependence between the selected variables. $r \in [-1,1]$, where $r = 1$ and $r = -1$ represent the perfect (monotonic) positive and negative correlation, respectively. It is given by

$$r = \frac{Cov[R(X),R(Y)]}{\sigma_{R(X)}\sigma_{R(Y)}}, \tag{4}$$

where $Cov[R(X),R(Y)]$ is the covariance of the ranked variables, and $\sigma_{R(X)}$ and $\sigma_{R(Y)}$ are their standard deviations. Additionally, p-values are calculated to determine the significance of the observed correlations. Both, the rank correlation coefficients (r) and the p-values help to identify the significant correlations between the variables in each cluster and, thus, set-up the DAG of the BN for that cluster.

The rank correlation coefficients for the available data are presented in Table 1(a), whereas Table 1(b) represents the rank correlation coefficients for the 6th cluster exemplarily.

Table 1. (a) Empirical rank correlation matrix for the total data set; (b) Empirical rank correlation matrix for the 6th cluster.

(a)

r	H_S	T_P	θ	c_X	c_Y
H_S	1.000	0.505	0.182	0.304	-0.130
T_P		1.000	0.154	0.532	0.058
θ			1.000	0.189	-0.335
c_X				1.000	-0.618
c_Y					1.000

(b)

	H_S	T_P	θ	c_X	c_Y
H_S	1.000	0.516	0.010	-0.040	0.194
T_P		1.000	0.006	0.098	-0.043
θ			1.000	-0.162	0.015
c_X				1.000	0.164
c_Y					1.000

4.3. Bayesian Network structure

In this Section, the setup of the DAG of the BN per cluster is presented. For this, the underlying physics, but also the rank correlation coefficients and the corresponding p-values are considered. The rank correlation matrix of the individual BN should approximate the empirical rank correlation matrix per cluster.

Depending on the direction of the surface waves and currents, the currents can influence the waves (see e.g. Rijnsdorp et al., 2023; Kumar and Hayatdavoodi, 2023). Consequently, for the DAGs for each BN, c_X has no parent nodes. If there is no significant correlation between θ and c_X, θ also does not have a parent node. Given that H_S is the main influence for the loads on the mooring lines, H_S does not have any child nodes. Based on these physical principles, the nodes are connected through arcs for significant correlations, until the rank correlation matrix of the BN approximates the empirical correlation matrix. Thus, arcs for pairs where the p-value is slightly above 0.05 are added. For the first cluster, this approach results in two independent BN's. For sake of simplicity, the two BN's are connected by an arc between variables with the lowest p-value. Additionally, two out of the total 7 clusters have variables not connected to the DAG.

Figure 3 shows the structure of the BN for the 6th cluster as an example. r_{ij} indicates the rank correlation coefficients between two variables (see Table 1 (b)). Note however that the correlation coefficient of variable 4 and 5 (r_{45}) is not the same as the conditional rank correlation coefficient between these variables given that variable 1 is known ($r_{45|1}$) (see Hanea et al. (2006) for further information).

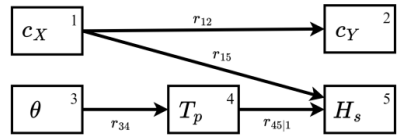

Fig. 3. Structure of the copula-based Bayesian Network for the 6th cluster.

4.4. Model validation

When building a BN, two hypotheses must be validated. Firstly, the dependence between selected variables is accurately described by the Gaussian copula assumption. Therefore, the Cramér-von Mises statistic (CvM) is applied (Genest et al., 2009) for each pair of variables. The CvM statistic is based on the sum of squared differences between the empirical and parametric joint cumulative distribution function given by the copula model. Next to the Gaussian copula, the Frank, Gumbel and Clayton copula are considered, of which the latter two are characterised by tail dependences. For most of the variable pairs , the Gaussian or Frank copula are found to be the best fit, being both symmetrical models (without tail dependence). For some pairs with low correlation, the Clayton or Gumbel copula models are selected as a better fit, but asymmetries are not found to be dominant when inspecting visually the dependence.

Secondly, the d-calibration score (Moráles-Napoles et al., 2013; Moráles-Napoles et al., 2014) is employed to assess how well the DAG of the BN represents the dependence structure between variables. This score measures the dissimilitude between two correlation matrices, where a score of 1 indicates identical matrices and the score approaches 0 if the matrices differ from each other elementwise. The d-calibration score is based on the Hellinger distance. For the proposed DAG for each cluster, the empirical rank correlation matrix is compared with the rank correlation matrix of the fully saturated BN, which represents the best possible model in which all random variables are connected to each other. The d-calibration scores are above 0.93, indicating that the suggested DAGs are suitable to represent the dependence structure.

4.5. Performance assessment

Here, the predictive power of the BN models is assessed through in-sample simulations. The results of the 6th cluster are presented as an example (the structure is presented in Figure 3).

To assess the model performance, the empirical data set is randomly split in half. The first half of the empirical data set is used to construct the BN. Note that the structure of the DAG was initially built based on the entire available dataset. The second half of the empirical data set is reserved for validation purposes.

To perform the validation, conditional samples are drawn from the BN (predicted) and compared against the reserved half of the empirical dataset (measured). The results for observed $H_S|c_X, \theta, T_P$ against the predicted

$H_S|c_X, \theta, T_P$ are shown in Figure 4. A good agreement can be seen; the BN slightly underestimates H_S and a trend of overestimating for H_S > 4.5 m can be observed.

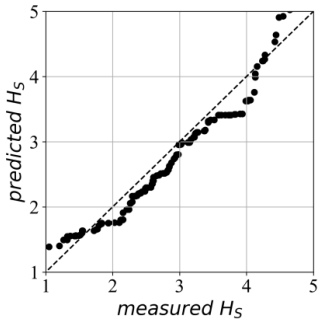

Fig. 4. Comparison between measured and estimated H_S using the BN model from the 6th cluster.

The coefficient of determination, R^2 is used to quantify the goodness of fit. $0 \leq R^2 \leq 1$ estimates the percentage of the variance explained by the model and is defined as

$$R^2 = 1 - \frac{\sum_i (y_i - f_i)^2}{\sum_i (y_i - \bar{y}_i)^2}, \tag{5}$$

where y_i are the observations, f_i the predictions and $\bar{y}_i$ the mean of observations. For H_S, R^2 is determined as 0.95. For the other variables of this cluster, the R^2 scores are above 0.93, except for cy (0.85). Generally, it can be said that this BN (see Figure 3) is a satisfactory model for this cluster.

5. Load analysis

For each of the seven clusters, 10,000 random samples are drawn from the individual BN's. Based on these samples, the flow velocity of waves at 3 m below MSL is calculated via linear wave theory (see Section 3). For both waves and currents, the in-line component of the flow velocity in relation to the structure orientation is determined. Then, the Morison loads per unit length are calculated for the mooring rope, using equation (2). The diameter of the rope is set to $D = 0.091$ m, $C_D = 2.2$ and the water density $\rho = 1025$ kg/m³. Using the calculated Morison loads, an exceedance curve is built, as shown in Figure 5. The results of cluster 2 and 4 present significantly higher loads compared to the other clusters. The reason is that these clusters present higher H_S and T_P values in comparison with the other clusters, while the differences for the current velocities are minor.

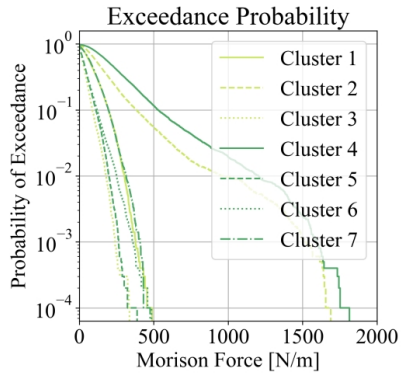

Fig. 5. Exceedance probability of the Morison force for each cluster.

The calculated load per cluster induced by waves and currents on the mooring lines independent from the structure do not exceed 1.8 kN. A few studies do exist, which investigated the loads in the mooring lines and anchors of a similar structure for mussel cultivation. (Gagnon and Bergeron, 2017) observed a maximum load in the anchors of 0.6 kN for submerged mussel long-line in less harsh environment. (Cheng et al., 2020) measured and calculated loads in the mooring lines of a similar structure under tide flow of between 9 and 10 kN, while (Stevens et al., 2007) observed loads of 1.2 kN in the mooring lines induced by tide only. Thus, the loads calculated here seem to be reasonable. Note however that these studies indicate the measured loads in the mooring lines and anchors, while the present study gives a first estimate of the horizontal loads on the mooring lines, independent from the remaining structure, induced by wave and current flow.

6. Conclusions

In this study, forces on the mooring lines of a seaweed cultivation structure are probabilistically characterised. This was done by calculating the loads on the rope due to wave and current velocities using the Morison equation. As available data is limited, Bayesian Networks were built to obtain more data while accounting for the dependence structure present in observations. To capture the compositions of different wave and current components, the available data was divided into 7 clusters by using the k-means++ algorithm. Research recently done in this direction indicates that a selection of wave and current flows parallel to the structure is most relevant. This conservative approach does not change the general approach described in this study. Here, BN's per cluster were built and validated via d-calibration score and in-sample performance assessment. It was found that copula-based BN's are a suitable technique for modelling the uncertainty of extremes in this case study and thus, can be used as input for the Morison equation to characterise the uncertainty of the loads. Regarding the load assessment, two clusters are found to present higher loads, due to higher H_S and T_P, compared to the other clusters. Further investigation is needed whether clustering the empirical data into two groups is sufficient. The calculated loads seem reasonable in comparison with measured loads from literature for comparable structures. Future research will focus on improving the estimation of the loads and dynamics of the studied structure and analysing the influence of accounting tail dependence in the joint distribution by using vine-copula models.

Acknowledgements

The first and third author were financially supported by the European Union's Horizon 2020 Research and Innovation Programme under Grant Agreement no 862915.

References

Airy, G. B. 1849. Tides and Waves. Encyclopædia metropolitana. London, 241-396.

Akaike, H. 1974. A new look at the statistical model identification. IEEE Transactions on Automatic Control AC-19, 716-723.

Araújo, R., Vázquez Calderón, F., Sánchez López, J., Azevedo, I.C., Bruhn, A., Fluch, S., Garcia Tasende, M., Ghaderiardakani, F., Ilmjärv, T., Laurans, M., Mac Monagail, M., Silvio, M., Peteiro, C., Rebours, C., Stefansson, T., Ullmann, J. 2021. Current status of the algae production industry in Europe: an emerging sector of the blue bioeconomy. Front. Mar. Sci. 7, 626389.

Arthur, D. and Vassilvitskii, S. 2007. k-means++: the advantages of careful seeding. ACM-SIAM Symposium on Discrete Algorithms.

Boderskov, T., Rasmussen, M.B., Bruhn, A. 2023. Upscaling cultivation of Saccharina latissima on net or line systems; comparing biomass yields and nutrient extraction potentials. Frontiers in Marine Science 10.

Booij, N., Ris, R. C., Holthuijsen, L. H. 1999. A third generation wave model for coastal regions. Part 1. Model description and validation, J. Geophys. Res. 104(C4), 76497666.

Buck, B. H., Krause, G., Michler-Cieluch, T., Brenner, M., Buchholz, C.M., Busch, J.A., Fisch, R., Geisen, M., Zielinski, O. 2008. Meeting the quest for spatial efficiency: Progress and prospects of extensive aquaculture within offshore wind farms. Helgoland Marine Research 62, 269–281.

Camus, P. Tomás, A., Díaz-Hernández, G., Rodríguez, B., Izaguirre, C., Losada, I. 2019. Probabilistic assessment of port operation downtimes under climate change. Coastal Engineering 147, 12–24.

Chakrabarti, S. K. 2005. Handbook of offshore engineering Vol. 1. s.l.: Elsevier.

Cheng, W., Sun, Z., Liang, S. Liu, B. 2020. Numerical model of an aquaculture structure under oscillatory flow. Aquacultural Engineering 89, 102054.

De Korte, E., Castelle, B., Tellier, E. 2021. A Bayesian network approach to modelling rip-current drownings and shore-break wave injuries. Natural Hazards and Earth System Sciences. 21. 2075-2091.

Deltares (2023). D-FLOW Flexible Mesh. User Manual, Deltares.

Feng, D., Meng, A., Wang, P., Yao, Y., Gui, F. 2021. Effect of design configuration on structural response of longline aquaculture in waves. Applied Ocean Research 107.

Gagnon, M., and Bergeron, P. 2017. Observations of the loading and motion of a submerged mussel longline at an open ocean site. Aquacultural Engineering, Elsevier B.V. 78, 114–129.
Geisler, R., Schulz, C., Michl, S., Strothotte, E. 2018. Feasbility study: Offshore-Aquakultur am Standort der Forschungsplattform FINO3.
Genest, C., Rémillard, B. and Beaudoin, D. 2009. Goodness-of-fit tests for copulas: A review and a power study. Insurance: Mathematics and Economics 44, 199–213.
Hanea, A.M., Kurowicka, D., Cooke, R.M. 2006. Hybrid Method for Quantifying and Analyzing Bayesian Belief Nets. Qual. Reliab. Engng. Int., 22, 709-729.
Joe, H. 2015. Dependence Modeling with Copulas. Monographs on Statistics and Applied Probability, 134. Boca Raton: CRC Press.
Kerrison, P. D., Stanley, M. S., Edwards, M. D., Black, K. D., Hughes, A. D. 2015. The cultivation of European kelp for bioenergy: Site and species selection. Biomass & Bioenergy 80, 229-242.
Kumar, A., Hayatdavoodi, M. 2023. Effect of currents on nonlinear waves in shallow water. Coastal Engineering. 181:104278-104278.
Maar, M., Holbach, A., Boderskov, T., Thomsen, M., Buck, B.H., Kotta, J., Bruhn, A. 2023. Multi-use of offshore wind farms with low-trophic aquaculture can help achieve global sustainability goals. Commun Earth Environ 4, 447.
Mares-Nasarre, P., Gracía-Maribona, J., Mendoza-Lugo, M.A., Morales-Nápoles, O. 2023. A copula-based Bayesian Network to model wave climate multivariate uncertainty in the Alboran sea. Proceeding of the 33rd European Safety and Reliability Conference. 1053-1060.
Mendoza-Lugo, M. A., Morales-Nápoles, O., Delgado-Hernández, D. J. 2022. A non-parametric bayesian network for multivariate probabilistic modelling of weigh-in-motion system data. Transportation Research Interdisciplinary Perspectives 13, 100552.
Mendoza-Lugo, M. A. and Morales-Nápoles, O. 2023. Version 1.3-Banshee – A MATLAB toolbox for Non-Parametric Bayesian Networks. SoftwareX 23, ISSN 23527110.
Morales-Nápoles, O., Hanea, A. M., Worm, D. 2013. Experimental results about the assessments of conditional rank correlations by experts: Example with air pollution estimates. In Proceedings 22nd European Safety and Reliability Conference: Safety, Reliability and Risk Analysis: Beyond the Horizon, ESREL 2013, Amsterdam, the Netherlands, 29–9 to 2–10. Taylor & Francis Group, London.
Morales-Nápoles, O., Delgado-Hernández, D. J., DeLeón-Escobedo, D., Arteaga-Arcos, J. C. 2014. A continuous bayesian network for earth dams' risk assessment: methodology and quantification. Structure and Infrastructure Engineering 10(5), 589–603.
Morison, J. R., O'Brien, M. P., Johnson, J. W., Schaaf, S. A. 1950. The force exerted by surface waves on piles. Petroleum Trans. AIME 189 149-189.
Pedregosa, F., Varoquaux, G., Gramfort, A., Michel, V., Thirion, B., Grisel, O., Blondel, M. , Prettenhofer, P. ,Weiss, R., Dubourg, V., Vanderplas, J., Passos, A., Cournapeau, D., Brucher, M., Perrot, M., Duchesnay, E. 2011. Scikit-learn: Machine Learning in Python. Journal of Machine Learning Research. 12. 2825-2830.
Plew, D. R., Stevens, C. L., Spigel, R. H., Hartstein, N. D. 2005. Hydrodynamic implications of large offshore mussel farms. IEEE Journal of Oceanic Engineering 30(1), 95-108.
Rijnsdorp, D. P., van Rooijen, A., Reniers, A., Tissier, M., de Wit, F., Zijlema, M. 2024. Including the effect of depth-uniform ambient currents on waves in a non-hydrostatic wave-flow model. Coastal Engineering. 187, 104420.
Santjer, R., Mares-Nasarre, P. ,El Serafy, G., Morales-Nápoles, O. 2023. A Case Study of Ecological Suitability of Mussel and Seaweed Cultivation using Bivariate Copula Functions. Proceeding of the 33rd European Safety and Reliability Conference. 1877-1884.
Spearman, C. 1987. The proof and measurement of association between two things. The American Journal of Psychology 100, 441–71.
Stevens, C. L., Plew, D. R., Smith, M. J., and Fredriksson, D. W. 2007. Hydrodynamic Forcing of Long-Line Mussel Farms: Observations. Journal of Waterway, Port, Coastal, and Ocean Engineering 133(3), 192–199.
Stevens, C. L., Plew, D. R., Hartstein, N., Fredriksson, D. 2008. The physics of open-water shellfish aquaculture. Aquacultural Enginering 38(3), 145-160.
Strothotte, E., Jaeger, M., Pforth, J., De-Clercq, A., Stechele, B., Nevejan, N., Knoop, J., Kerkhove, T., Petit, S., Vandercammen, D., Pilgrim, L., Pribadi, A., Fernandez, G. V., Lataire, E., Groenendaal, B., Drigkopoulou, I., Vlacheas, P., Demestichas, P., Tzanettis, I., Foteinos, V., Trichias, K., Brouwers, E., Sørensen, H., Triest, J. 2021. Deliverable 7.2: Blueprint for the offshore site operation (european united project, grant agreement no 862915).
Sumer, B. M. and Fredsøe, J. 2006. Hydrodynamics around cylindrical structures - Revised Edition. Denmark : World Scientific, 2006.
Yong, W. T. L., Thien, V. Y., Rupert, R., Rodrigues, K. F. 2022. Seaweed: A potential climate change solution. Renewable and Sustainable Energy Reviews 159
Zijl, F., Zijlker, T., Laan, S., Groenenboom, J. 2023. 3D DCSM FM: A sixth-generation model for the NW European Shelf. Technical Report, Deltares.